2015 IEEE Conference on Control Applications (CCA)
Part of 2015 IEEE Multi-Conference on Systems and Control
September 21-23, 2015. Sydney, Australia

A New Continuous Velocity Observer Formulation for a Class of Uncertain Nonlinear Mechanical Systems

Alper Bayrak[1], Enver Tatlicioglu[2⋆], Erkan Zergeroglu[3], and Meryem Deniz[2]

Abstract— **In this study, we present a smooth robust velocity observer for a class of uncertain nonlinear mechanical systems. The smoothness of the observers is guaranteed by utilizing hyperbolic tangent function as opposed to signum-type functions applied in most robust and sliding mode observers found in the literature. The proposed observer does not require *a priori* knowledge of an upper bound of the uncertain system dynamics and introduces a time–varying observer gain for uncertainty compensation. Practical stability of the observer error is ensured via Lyapunov-type stability analysis. Numerical simulation studies backed up by experimental results are presented to illustrate the performance of the proposed observer.**

I. Introduction

Most of the commercially available mechanical systems (especially industrial robot manipulators) are not equipped with a physical sensor to measure the velocities of the system. In the lack of sensory information for the velocities, in the literature, the two common ways to obtain the velocity data are either by filtering the position data [1] or by designing an observer [2], [3], [4]. In filter–based approaches, usually a filter is designed to approximate the behavior of a differentiator over a range of frequencies which in most cases results in extra numerical noise insertion to the overall system. On the other hand, use of observers for velocity estimation as in [2], [3], and [4] avoids the aforementioned drawback of filter–based techniques. While most of these velocity observers require the dynamical model of the mechanical system to be partially or exactly known [5], [6], there are robust observers [3], [4] that require only the upper bounds of the uncertain functions in the dynamical model. These robust observers can roughly be grouped as the ones that utilize signum function in their designs (*i.e.*, sliding mode observers or their modifications) [3], [4], [7], [8], [9], [10], [11] and the ones that require higher observer gains (*i.e.*, high–gain observers) [12], [13], [14]. While the discontinuous nature of the signum function is considered to be useful in the stability analysis, researchers seeked for alternatives to replace them especially for some implementations where smoothness is required. The commonly utilized alternatives of the signum function are the hyperbolic tangent function and the saturation function. However, most of the past works did not analyze the consequences of this modification with mathematical rigor.

The lack of mathematical proof of utilizing hyperbolic tangent function in lieu of signum function in observer designs motivated this work. Specifically, a novel continuous velocity observer for nonlinear mechanical systems is aimed. In the literature, hyperbolic tangent function is usually utilized as a continuous approximation of the signum function. Specifically, the approximation $\tanh(\kappa s(t)) \approx \text{sgn}(s(t))$ is considered for some "big" positive constant $\kappa \in \mathbb{R}$ and for some time–varying function $s(t) \in \mathbb{R}$. However, a common approach in the literature is to conduct the stability analysis for the signum function (to make use of its discontinuous nature to reject uncertainties) and to utilize hyperbolic tangent function for numerical verification (when discontinuity is a concern in the implementation). In a seemingly novel departure from the existing results in the literature, in this paper, hyperbolic tangent function is utilized in the observer design and its associated analysis is presented. It is also noted that, unlike the above approximation, in our design, we used $\kappa = 1$ so hyperbolic tangent function is applied to the argument of the signum function directly. The proposed observer design includes a time–varying observer gain to avoid the need of *a priori* knowledge of the upper bounds of the uncertain mechanical system dynamics. Lyapunov type stability analysis techniques are utilized to demonstrate practical tracking (*i.e.*, the velocity observer error can be driven to the vicinity of the origin that can be adjusted to be arbitrarily small). The performance of the proposed observer was demonstrated by both numerical simulations and experiments performed on a twin rotor system.

The rest of the paper is organized in the following manner. The plant model considered in this work is presented in Section II, while the observer formulation and the stability analysis are presented in Sections III and IV, respectively. Numerical studies performed on a two link robot manipulator are presented in Section V-A, and experimental results obtained from a twin rotor system are presented in Section V-B. Finally concluding remarks are given in Section VI.

II. Plant Model

The mechanical system model considered in this work is a second order nonlinear dynamical equation in the form

$$\ddot{x} = h(x, \dot{x}) + G(x, \dot{x})u \tag{1}$$

[1] Electrical & Electronics Engineering, Abant Izzet Baysal University, Bolu, 14280 Turkey. E–mail: alperbayrak@ibu.edu.tr
[2] Department of Electrical & Electronics Engineering, Izmir Institute of Technology, Urla, Izmir, 35430 Turkey. E–mails: [envertatlicioglu,meryemdeniz]@iyte.edu.tr
[3] Department of Computer Enginering, Gebze Technical University, Gebze, Kocaeli, Turkey. E–mail: e.zerger@gyte.edu.tr
⋆ Correspondence should be addressed to E. Tatlicioglu (Phone: +90 (232) 7506536; Fax: +90 (232) 7506599).
E. Tatlicioglu, E. Zergeroglu and M. Deniz are funded by The Scientific and Technological Research Council of Turkey via grant number 113E147.

where $x(t) \in \mathbb{R}^n$ is the position (*i.e.*, the output) with $\dot{x}(t)$, $\ddot{x}(t) \in \mathbb{R}^n$ denoting velocity and acceleration of the mechanical system, respectively, $u(t) \in \mathbb{R}^n$ is the control input, $h(x, \dot{x}) \in \mathbb{R}^n$ and $G(x, \dot{x}) \in \mathbb{R}^{n \times n}$ are uncertain nonlinear functions of position and velocity of the mechanical system.

The subsequent observer development requires the mechanical system model in (1) to satisfy the following standard assumptions (see [15] for the precedence of these assumptions).

Assumption 1: The nonlinear functions $h(x, \dot{x})$, $G(x, \dot{x})$, and the control input $u(t)$ are $\mathcal{C}^1$.

Assumption 2: The control input and its time derivative are bounded functions of time [*i.e.*, $u(t)$, $\dot{u}(t) \in \mathcal{L}_\infty$].

Assumption 3: The system output $x(t)$ and its time derivative $\dot{x}(t)$ remain bounded for all time [*i.e.*, $x(t)$, $\dot{x}(t) \in \mathcal{L}_\infty$].

III. Observer Design

Our objective is to design a continuous observer to estimate the velocity of the mechanical system. Mathematically, a velocity observer signal, denoted by $\dot{\hat{x}}(t) \in \mathbb{R}^n$, will be designed to observe $\dot{x}(t)$ while ensuring the velocity observer error, defined as $\dot{\tilde{x}}(t) \triangleq \dot{x}(t) - \dot{\hat{x}}(t)$, approach to a finite and acceptable region around the origin. The design problem is restricted by the constraint that the right–hand side of the system model in (1) being uncertain.

To achieve this objective, the subsequent stability analysis allowed us to design the velocity observer as

$$\dot{\hat{x}} = p + (K + I_n)\tilde{x} \tag{2}$$

where $K \in \mathbb{R}^{n \times n}$ is a positive definite, diagonal, constant observer gain matrix, $I_n \in \mathbb{R}^{n \times n}$ is the standard identity matrix, and $\tilde{x}(t) \in \mathbb{R}^n$ is the position observer error defined as

$$\tilde{x} \triangleq x - \hat{x}. \tag{3}$$

The term $p(t) \in \mathbb{R}^n$ in (2) denotes an auxiliary filter signal updated according to

$$\dot{p} = K\tilde{x} + \hat{\beta} Tanh(\tilde{x}) \tag{4}$$

where $\hat{\beta}(t) \in \mathbb{R}^{n \times n}$ is a positive definite, diagonal, time–varying observer gain matrix and $Tanh(\tilde{x}) \in \mathbb{R}^n$ is the vector form of the hyperbolic tangent function defined as

$$Tanh(\tilde{x}) \triangleq [\tanh(\tilde{x}_1), ..., \tanh(\tilde{x}_n)]^T \tag{5}$$

for $\tilde{x} \triangleq [\tilde{x}_1, ..., \tilde{x}_n]^T$. We design the entries of the time–varying observer gain matrix $\hat{\beta}(t)$ to have the following form

$$\hat{\beta}_i(t) = \ln(\cosh(\tilde{x}_i(t))) + \int_0^t \tilde{x}_i(\tau) \tanh(\tilde{x}_i(\tau)) d\tau \tag{6}$$

$\forall i = 1, \cdots, n$. Notice from (6) that $\hat{\beta}_i(t) > 0 \ \forall t$.

Remark 1: The main difference between the velocity observer in this paper and the velocity observer in [15] is that we used hyperbolic tangent function instead of the signum function. An important difference of the proposed velocity observer from the one in [15] is that, as opposed to the constant observer gain K_2 in (45) of [15], we designed a time–varying observer gain when multiplying the hyperbolic tangent function [*i.e.*, $\hat{\beta}(t)$ in (4)].

IV. Stability Analysis

In this section, the stability of the velocity observer design in (2)–(6) will be presented. To facilitate the stability analysis, we define a filtered version of the position observer error, denoted by $r(t) \in \mathbb{R}^n$, as follows

$$r \triangleq \dot{\tilde{x}} + \tilde{x}. \tag{7}$$

Notice that, since the velocity observer error $\dot{\tilde{x}}(t)$ is unavailable, the filtered observer error $r(t)$ is unavailable as well. Taking the time derivative of (7) yields

$$\dot{r} = \ddot{x} - \ddot{\hat{x}} + \dot{\tilde{x}} \tag{8}$$

where the second time derivative of (3) was utilized. After taking the time derivative of (2) and substituting (4), we reach

$$\ddot{\tilde{x}} = Kr + \dot{\tilde{x}} + \hat{\beta} Tanh(\tilde{x}) \tag{9}$$

where (7) was utilized. Substituting (1) and (9) into (8) yields the dynamics for the filtered observer error to be obtained in the following form

$$\dot{r} = -Kr + N - \hat{\beta} Tanh(\tilde{x}) \tag{10}$$

where the auxiliary signal $N(t) \in \mathbb{R}^n$ is defined as

$$N \triangleq h + Gu. \tag{11}$$

It is highlighted that, based on Assumptions 1, 2 and 3, it is clear that $N(t)$ and $\dot{N}(t)$ are bounded functions of time.

An auxiliary function $V_L(t) \in \mathbb{R}$ is defined as

$$V_L \triangleq \zeta_L - L \tag{12}$$

where $L(t) \in \mathbb{R}$ is given as

$$L \triangleq \int_0^t r^T(\tau) \left[N(\tau) - \beta Tanh(\tilde{x}(\tau)) \right] d\tau \tag{13}$$

with $\beta \in \mathbb{R}^{n \times n}$ being a positive definite diagonal constant matrix, and $\zeta_L \in \mathbb{R}$ is a constant given as follows

$$\zeta_L \triangleq \sum_{i=0}^{n} \beta_i \left(\ln \left[\cosh(\tilde{x}_i(0)) \right] + 1 \right) - \tilde{x}^T(0) N(0). \tag{14}$$

We are now ready to state the following lemma whose results will later be utilized in the proof of the main theorem.

Lemma 1: When

$$\forall \|\tilde{x}\| \geq d(\varepsilon) \tag{15}$$

which can alternatively be stated as $\tilde{x}(t)$ being outside of a hyperball around the origin, the auxiliary term $V_L(t)$ can be lower bounded in the sense that

$$V_L(t) \geq 0 \tag{16}$$

provided that the entries of β satisfy

$$\beta_i > \frac{1}{\varepsilon} \left(\|N_i\|_\infty + \left\| \dot{N}_i \right\|_\infty \right) \tag{17}$$

where subscript i denotes the entries of a vector or a diagonal matrix, the notation $\|\cdot\|_\infty$ denotes the supremum of a time–varying signal, and ε is a positive design parameter which specifies the radius of the hyperball $d(\varepsilon)$. Alternatively, for

the region in (15), provided (17) is satisfied, from (12) and (13), we can obtain

$$\zeta_L \geq \int_0^t r^T(\tau)\left[N(\tau) - \beta Tanh\left(\tilde{x}(\tau)\right)\right] d\tau. \quad (18)$$

Proof: Substituting the definition of $r(t)$ in (7) into (13) yields

$$\begin{aligned} L &= \int_0^t \tilde{x}^T(\tau)\left(N(\tau) - \beta Tanh\left(\tilde{x}(\tau)\right)\right) d\tau \\ &+ \int_0^t \frac{d\tilde{x}^T(\tau)}{d\tau} N(\tau)\, d\tau \\ &- \int_0^t \frac{d\tilde{x}^T(\tau)}{d\tau} \beta Tanh\left(\tilde{x}(\tau)\right) d\tau. \end{aligned} \quad (19)$$

After evaluating the last integral and integrating the second one by parts, we can obtain

$$\begin{aligned} L &= \int_0^t \tilde{x}^T(\tau)\left(N(\tau) - \frac{dN(\tau)}{d\tau} - \beta Tanh\left(\tilde{x}(\tau)\right)\right) d\tau \\ &+ \tilde{x}^T(t) N(t) - \sum_{i=1}^{n} \beta_i \left(\ln\left(\cosh\left(\tilde{x}_i(t)\right)\right) + 1\right) \\ &+ \sum_{i=1}^{n} \beta_i \left(\ln\left(\cosh\left(\tilde{x}_i(0)\right)\right) + 1\right) - \tilde{x}^T(0) N(0). \end{aligned} \quad (20)$$

Now, after using the property $\tilde{x}^T(t) Tanh\left(\tilde{x}(t)\right) \geq 0$, we can upper bound the right–hand side of (20) as

$$\begin{aligned} L &\leq \int_0^t \sum_{i=1}^{n} |\tilde{x}_i(\tau)| \left(\|N_i(\tau)\|_\infty + \left\| \tfrac{dN_i(\tau)}{d\tau} \right\|_\infty \right. \\ &- \left. \beta_i \left|\tanh\left(\tilde{x}_i(\tau)\right)\right| \right) d\tau \\ &+ \|\tilde{x}(t)\| \|N(t)\|_\infty - \sum_{i=1}^{n} \beta_i \left(\ln\left(\cosh\left(\tilde{x}_i(t)\right)\right) + 1\right) \\ &+ \sum_{i=1}^{n} \beta_i \left(\ln\left(\cosh\left(\tilde{x}_i(0)\right)\right) + 1\right) - \tilde{x}^T(0) N(0) \end{aligned} \quad (21)$$

where $\sum_{i=1}^{n} \beta_i$ was added and subtracted. When $\|\tilde{x}(t)\| \geq d(\varepsilon)$ and the entries of β satisfy (17), the integral term on the right–hand side of (21) (the first two lines) takes negative values. Applying the fact [16]

$$\frac{1}{\lambda}\left(\sum_{i=0}^{n} \ln\left(\cosh\left(\tilde{x}_i(t)\right)\right) + 1\right) - \|\tilde{x}\| > 0 \ \forall \lambda \in (0,1) \quad (22)$$

when $\varepsilon < \|Tanh(\tilde{x}(t))\|$ is satisfied, the third line of (21) would also be negative. Utilizing the definition of the constant ζ_L in (14) along with the above facts, results in $V_L(t)$ being positive when $\varepsilon < \|Tanh(\tilde{x}(t))\|$. In other words, $V_L(t)$ is positive if $\|\tilde{x}(t)\|$ is outside the hyperball $d(\varepsilon)$, whose radius can be adjusted using ε. ■

Remark 2: As presented in the proof of Lemma 1 and will be demonstrated in the proof of the main theorem, if $\varepsilon = 0$, then, it would be possible to drive the velocity observer error to zero. But as $\varepsilon \to 0$ then, from (17), it is clear that $\beta \to +\infty$. While this seems like a problem, as highlighted in Remark 1, β is not utilized in the observer design and instead the time–varying observer gain $\hat{\beta}(t)$ was introduced and utilized in (4).

Theorem 1: The velocity observer in (2)–(6) ensures ultimate asymptotic convergence of velocity observer error $\dot{\tilde{x}}(t)$ to a hyperball with an adjustable radius.

Proof: To prove this theorem, we define the following function

$$V \triangleq V_L + \frac{1}{2} r^T r + \frac{1}{2} \sum_{i=1}^{n} \tilde{\beta}_i^2 \quad (23)$$

where

$$\tilde{\beta}_i \triangleq \beta_i - \hat{\beta}_i \quad (24)$$

and $V_L(t)$ was previously defined in Lemma 1. Note that the expression in (23) is positive and lower bounded provided that $V_L(t) \geq 0$ [*i.e.*, when $\|\tilde{x}\| \geq d(\varepsilon)$ from Lemma 1] and thus on the same region satisfies

$$\alpha_1(\|w\|) \leq V(t,w) \leq \alpha_2(\|w\|) \quad \forall \|w\| \geq \|\tilde{x}\| \geq d(\varepsilon) \quad (25)$$

where $w(t) \in \mathbb{R}^{(2n+1)\times 1}$ is defined as

$$w \triangleq \left[\begin{array}{ccccc} r^T & \tilde{\beta}_1 & \ldots & \tilde{\beta}_n & \sqrt{V_L} \end{array}\right]^T. \quad (26)$$

Based on (23), the class $\mathcal{K}$ functions $\alpha_1(\|w\|)$ and $\alpha_2(\|w\|)$ are defined as

$$\alpha_1(\|w\|) \triangleq \frac{1}{2}\|w\|^2, \ \alpha_2(\|w\|) \triangleq \|w\|^2. \quad (27)$$

By taking the time derivative of (23), we obtain

$$\dot{V} = \dot{V}_L + r^T \dot{r} + \sum_{i=1}^{n} \tilde{\beta}_i \dot{\tilde{\beta}}_i. \quad (28)$$

By utilizing the time derivative of $V_L(t)$ in (12) along with the time derivative of $L(t)$ in (13), and substituting (10) into (28), we obtain

$$\begin{aligned} \dot{V} &= r^T(-N + \beta Tanh(\tilde{x})) \\ &+ r^T(-Kr + N - \hat{\beta} Tanh(\tilde{x})) + \sum_{i=1}^{n} \tilde{\beta}_i \dot{\tilde{\beta}}_i. \end{aligned} \quad (29)$$

Note that, from the time derivative of (6), we obtain

$$\dot{\tilde{\beta}}_i = r_i \tanh(\tilde{x}_i) \ \forall i = 1, \cdots, n. \quad (30)$$

After utilizing the time derivative of $\tilde{\beta}_i(t)$ in (24) along with (30), from (29), we reach

$$\dot{V} = r^T\left(\beta - \hat{\beta}\right) Tanh(\tilde{x}) - \sum_{i=1}^{n} \tilde{\beta}_i r_i \tanh(\tilde{x}_i) - r^T K r \quad (31)$$

and after considering the fact

$$r^T\left(\beta - \hat{\beta}\right) Tanh(\tilde{x}) = \sum_{i=1}^{n} r_i \tilde{\beta}_i \tanh(\tilde{x}_i) \quad (32)$$

we obtain

$$\dot{V} = -r^T K r \quad \forall \|w\| \geq \|\tilde{x}\| \geq d(\varepsilon). \quad (33)$$

From (23) and (33), it is clear that $V(t) \in \mathcal{L}_\infty$ and thus $r(t)$, $V_L(t)$, $\tilde{\beta}(t) \in \mathcal{L}_\infty$. From the definition of $r(t)$, the

error signals $\tilde{x}(t)$, $\dot{\tilde{x}}(t) \in \mathcal{L}_\infty$. From the structures of (23) and (33), it can be stated that the trajectories of velocity observer error $\dot{\tilde{x}}(t)$ starting from any given initial value will approach into the hyperball in (15) as time increases provided that (17) is satisfied. ■

V. Numerical Results

In this section, the performance of the proposed observer was demonstrated by numerical simulation and experimental results. First, a numerical simulation was performed on a two link robot manipulator model. Next, experiment results were obtained from a twin rotor system [17], [18].

A. Simulation Results

In this section, numerical simulations conducted on a two link robot manipulator model is presented. The equations of motion are as follows [14]

$$\begin{aligned} &\begin{bmatrix} H_{11} & H_{12} \\ H_{12} & H_{22} \end{bmatrix} \begin{bmatrix} \ddot{x}_1 \\ \ddot{x}_2 \end{bmatrix} \\ &+ \begin{bmatrix} -h\dot{x}_2 & -h(\dot{x}_1 + \dot{x}_2) \\ -h\dot{x}_1 & 0 \end{bmatrix} \begin{bmatrix} \dot{x}_1 \\ \dot{x}_2 \end{bmatrix} \\ &= (H_{11}H_{22} - H_{12}^2) \begin{bmatrix} 1 & 1 \\ 0 & 1 \end{bmatrix} \begin{bmatrix} u_1 \\ u_2 \end{bmatrix} \end{aligned} \tag{34}$$

where $x_1(t)$, $x_2(t) \in \mathbb{R}$ denote angular positions of joints and $u_1(t)$, $u_2(t) \in \mathbb{R}$ are the control inputs which were applied as $[u_1(t), u_2(t)]^T = [\sin(t), \cos(t)]^T$. In (34), H_{11}, H_{12}, H_{22} and h are defined as

$$H_{11} = a_1 + 2a_3 \cos(x_2) \tag{35}$$

$$H_{12} = a_2 + a_3 \cos(x_2) \tag{36}$$

$$H_{22} = a_2 \tag{37}$$

$$h = a_3 \sin(x_2) \tag{38}$$

where the values of the parameters were $a_1 = 3.473$, $a_2 = 0.193$ and $a_3 = 0.242$. We would like to highlight that the above modeling functions were only utilized to simulate the robot manipulator and they were not utilized in the observer design.

The robot manipulator is considered to be at rest at the initial positions of $x(0) = [\ 0.06 \quad 0.06\ ]^T(\text{deg})$. During the simulation, the observer gain was set to $K = \text{diag}\{10, 10\}$. The auxiliary filter signal in (4) was initiated from zero, and $\hat{x}(0) = [\ 57 \quad 57\ ]^T(\text{deg})$.

The actual velocity $\dot{x}(t)$ and the observed velocity $\dot{\hat{x}}(t)$ are shown in Figure 1. The velocity observer error $\dot{\tilde{x}}(t)$ is shown in Figure 2. The diagonal entries of the time–varying observer gain matrix $\hat{\beta}(t)$ are presented in Figure 3. From Figures 1 and 2, it is clear that the velocity observer is working accurately and the design objective was met.

B. Experimental Results

The proposed velocity observer was experimentally tested on a twin rotor system in our laboratory at Izmir Institute of Technology [17], [18]. Twin rotor system, which is a nonlinear system with significant cross coupling, resembles a helicopter model. The mechanical system which was used

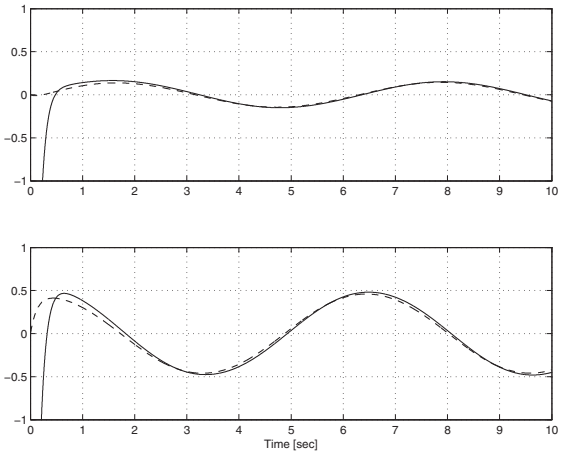

Fig. 1. The actual velocity $\dot{x}(t)$ (dashed) and the observed velocity $\dot{\hat{x}}(t)$.

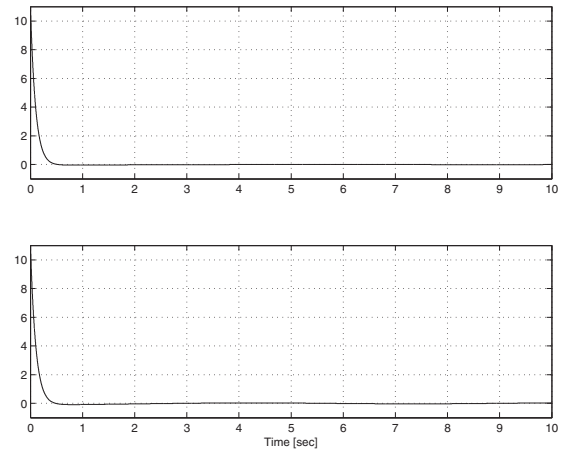

Fig. 2. The velocity observer error $\dot{\tilde{x}}(t)$.

in the experiment studies was built in our laboratory, and used as a test–bed for various control applications. The system consists of two rotors placed on a beam. Similar to a helicopter, position and velocity of the beam are controlled by changing the rotor velocities. The electronic sub–system consists of two motor drivers, two optical encoder readers, and a PC–to–device communication interface. The system sends yaw and pitch angles to PC and receives motor velocity information from PC via an RS232 port with a 56700 baud rate, and is controlled via the LabView software.

Researchers pursued several approaches to develop a dynamic model for the twin rotor system. Reviewing the literature reveals the dynamic model of a twin rotor system to be of the following form [19]

$$M\ddot{x} = f + u \tag{39}$$

where $x(t) \triangleq [x_p(t), x_y(t)]^T \in \mathbb{R}^2$ denoting pitch and yaw angles of the beam, $M(x) \in \mathbb{R}^{2\times 2}$, $f(x, \dot{x}) \in \mathbb{R}^2$ are uncertain nonlinear functions, $u(t) \in \mathbb{R}^2$ is the control

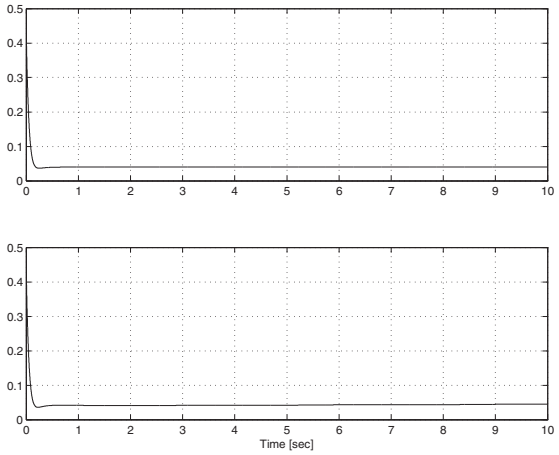

Fig. 3. The diagonal entries of the time–varying observer gain matrix $\hat{\beta}(t)$.

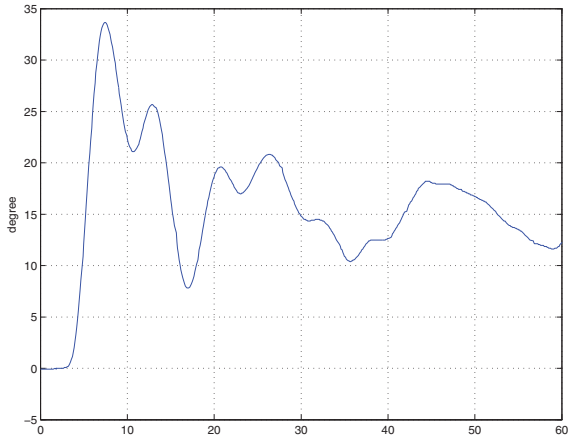

Fig. 4. Pitch angle $x_p(t)$.

input. In (39), $\dot{x}(t)$, $\ddot{x}(t) \in \mathbb{R}^2$ denote velocity and acceleration vectors, respectively. Notice that, choosing $G(x,\dot{x}) = M^{-1}(x)$, $h(x,\dot{x}) = M^{-1}(x) f(x,\dot{x})$ yields the model in (1).

During the experiment, the control input is designed as $u(t) = (1 - \exp(-t))[590, 750]^T + [10\sin(0.1\pi t), -150\sin(0.1\pi t)]^T$, and the observer gain matrices[1] were set to $K = diag(0.01, 0.0001)$ and $\hat{\beta} = diag(0.0016, 0.0002)$.

The pitch angle $x_p(t)$ and yaw angle $x_y(t)$ are shown in Figures 4 and 5, respectively. The pitch angle observer error $\tilde{x}_p(t)$ and the yaw angle observer error $\tilde{x}_y(t)$ are shown in Figures 6 and 7, respectively. Finally, the observed pitch velocity $\dot{\hat{x}}_p(t)$ and the observed yaw velocity $\dot{\hat{x}}_y(t)$ are shown in Figures 8 and 9, respectively. From Figures 6 and 7, it is clear that the observer design objective was met.

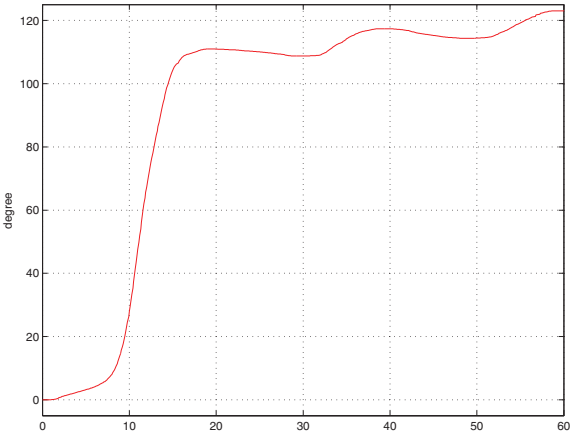

Fig. 5. Yaw angle $x_y(t)$.

VI. Conclusion

In this work, a new robust continuous velocity observer was designed for a class of uncertain nonlinear mechanical systems. The smoothness of the velocity observer was ensured via the use hyperbolic tangent function in the design. The design of the velocity observer differs from the similar observer techniques in the literature in the sense that, the proposed observer utilizes a time–varying observer gain for uncertainty compensation. Ultimate asymptotic stability of the observer error was ensured via Lyapunov–type stability analysis. Numerical simulations backed up with experimental results performed on a highly nonlinear system were presented to illustrate the performance of the proposed observer.

Current research is underway to make the proposed observer a fully self–tuning velocity observer by designing an adaptive update rule for the constant gain matrix K.

[1]For simplicity reasons, the time–varying observer gain matrix $\hat{\beta}$ was chosen as a constant.

References

[1] Y. X. Su, C. H. Zheng, P. C. Mueller, and B. Y. Duan, "A simple improved velocity estimation for low-speed regions based on position measurements only," *IEEE Trans. Contr. Syst. Technol.*, vol. 14, no. 5, pp. 937–942, 2006.

[2] S. Arimoto, V. Parra-Vega, and T. Naniwa, "A class of linear velocity observers for nonlinear mechanical systems," in *Proc. of Asian Control Conf.*, Tokyo, Japan, 1994, pp. 633–636.

[3] C. C. de Wit and J. Slotine, "Sliding observers for robot manipulators," *Automatica*, vol. 27, no. 5, pp. 859–864, 1991.

[4] A. Abdessameud and M. F. Khelfi, "A variable structure observer for the control of robot manipulators," *Int. J. Appl. Math. Compt. Sci.*, vol. 16, no. 2, pp. 189–196, 2006.

[5] A. Astolfi, R. Ortega, and A. Venkatraman, "A globally exponentially convergent immersion and invariance speed observer for mechanical systems with non-holonomic constraints," *Automatica*, vol. 46, no. 5, pp. 182–189, 2010.

[6] M. Namvar, "A class of globally convergent velocity observers for robotic manipulators," *IEEE Trans. Automat. Contr.*, vol. 54, no. 8, pp. 1956–1961, 2009.

[7] J. Davila, L. Fridman, and A. Levant, "Second-order sliding-mode observer for mechanical systems," *IEEE Trans. Automat. Contr.*, vol. 50, no. 11, pp. 1785–1789, 2005.

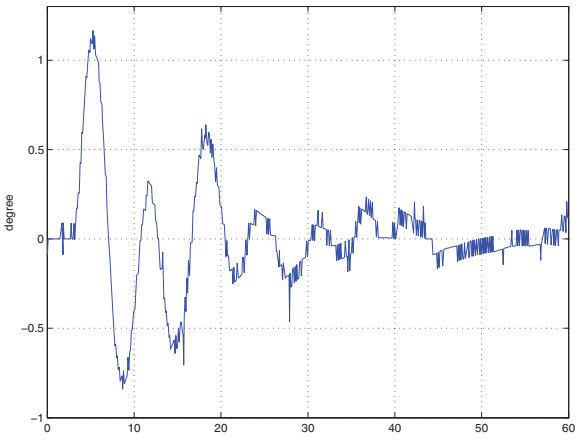

Fig. 6. Pitch angle observer error $\tilde{x}_p(t)$.

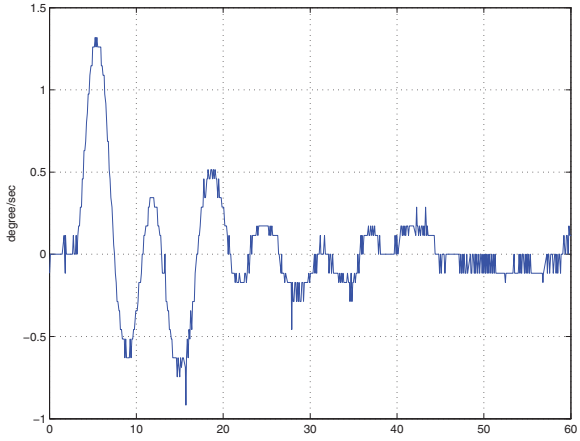

Fig. 8. Observed pitch velocity $\dot{\hat{x}}_p(t)$.

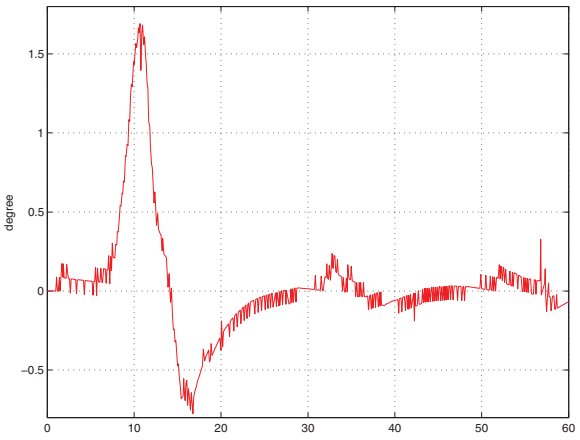

Fig. 7. Yaw angle observer error $\tilde{x}_y(t)$.

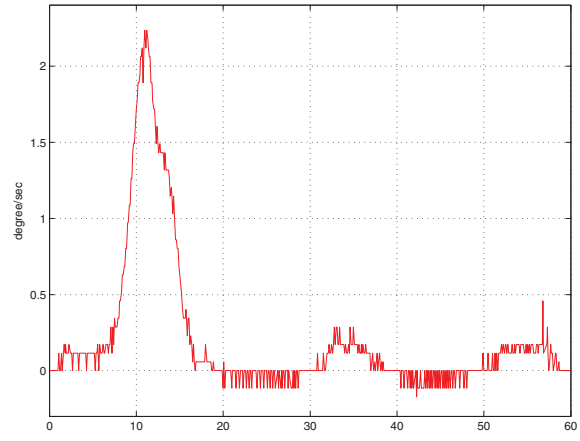

Fig. 9. Observed yaw velocity $\dot{\hat{x}}_y(t)$.

[8] J.-H. Choi, E. A. Misawa, and G. E. Young, "A study on sliding mode state estimation," *ASME J. Dynamic Systems, Measurement, and Control*, vol. 121, no. 6, pp. 255–260, 1999.

[9] Y. Xiong and M. Saif, "Sliding mode observer for nonlinear uncertain systems," *IEEE Trans. Automat. Contr.*, vol. 46, no. 12, pp. 2012–2017, 2001.

[10] D. M. Dawson, Z. Qu, and J. C. Carroll, "On the state observation and output feedback problems for nonlinear uncertain dynamic systems," *Systems and Control Letters*, vol. 18, no. 2, pp. 217–222, 1992.

[11] B. Walcott and S. Zak, "State observation of nonlinear uncertain dynamical systems," *IEEE Trans. Automat. Contr.*, vol. 32, no. 2, pp. 166–170, 1987.

[12] A. Teel and L. Praly, "Global stabilizability and observability imply semi global stabilizability by output feedback," *Systems and Control Letters*, vol. 22, no. 2, pp. 313–325, 1994.

[13] A. N. Atassi and H. K. Khalil, "A separation principle for the stabilization of a class of nonlinear systems," *IEEE Trans. Automat. Contr.*, vol. 44, no. 9, pp. 1672–1687, 1999.

[14] J. Chen, A. Behal, and D. Dawson, "Robust feedback control for a class of uncertain mimo nonlinear systems," *IEEE Trans. Automat. Contr.*, vol. 53, no. 2, pp. 591–596, 2008.

[15] B. Xian, M. de Queiroz, D. Dawson, and M. McIntyre, "A discontinuous output feedback controller and velocity observer for nonlinear mechanical systems," *Automatica*, vol. 40, no. 4, pp. 695 – 700, 2004.

[16] J. Dasdemir and E. Zergeroglu, "A new continuous high-gain controller scheme for a class of uncertain nonlinear systems," *Int. J. of Robust and Nonlinear Control*, vol. 25, no. 1, pp. 125–141, 2015.

[17] A. Bayrak, F. Dogan, E. Tatlicioglu, and B. Ozdemirel, "Design of an experimental twin-rotor multi-input multi-output system," *Computer Applications in Engineering Education*, vol. 23, no. 4, pp. 578–586, 2015.

[18] F. Dogan, "Design, Development and Control of a Twin Rotor System," Master's thesis, Izmir Institute of Technology, Izmir, Turkey, 2014.

[19] A. Rahideh and M. H. Shaheed, "Mathematical dynamic modelling of a twin-rotor multiple input multiple output system," *Proc. of Ins. of Mechanical Engineers Part I: J. Systems and Control Engineering*, vol. 221, pp. 89–101, 2007.